



40th European Rotorcraft Forum  
 Southampton, 2-5 September, 2014  
 Paper 83

# CFD-BASED SIMULATION OF HELICOPTER IN SHIPBORNE ENVIRONMENT

C. CROZON, R. STEIJL AND G.N. BARAKOS

CFD Laboratory, School of Engineering  
 University of Liverpool, L69 3GH, U.K.  
<http://www.liv.ac.uk/cfd>

[crozon@liverpool.ac.uk](mailto:crozon@liverpool.ac.uk), [rsteijl@liverpool.ac.uk](mailto:rsteijl@liverpool.ac.uk), [g.barakos@liverpool.ac.uk](mailto:g.barakos@liverpool.ac.uk)

## Abstract

The development of High Performance Computing and CFD methods have evolved to the point where it is possible to simulate complete helicopter configurations with a good accuracy. These capabilities have been applied to a variety of problems such as rotor/fuselage and main/tail rotors interactions, helicopter performance in hover and forward flight, rotor design, etc. The GOA-HEAD project is a good example of a coordinated effort to validate CFD for such helicopter configurations. These simulations, however, have been limited to steady flight problems. The present work addresses the problem of simulating manoeuvring flights by coupling the CFD code HMB2 with a versatile multi-body grid motion method and a Helicopter Flight Mechanics (HFM) method. The formulation of the CFD has been adapted to the change in frame of reference used for the calculations. After a discussion of the previous work carried out on the subject and a description of the methods used, validation of the CFD for ship airwake, and rotorcraft at low advance ratio flight are presented. Finally, the results obtained for various test cases using the new method are presented and discussed.

## NOMENCLATURE

$A B C$	Matrices of the linear model
$CG$	Helicopter Center of Gravity
$F_x F_y F_z$	Global forces at CG
$L M N$	Global moments at CG
$p q r$	Body rotation rates
$u v w$	Body velocities
$x_e y_e z_e$	Body position in earth-fixed FoR
$\Psi$	Rotor azimuth
$\phi \theta \psi$	Body attitude angles
$\theta_0^M \theta_0^T$	Main and tail rotor collective
$\theta_{1s} \theta_{1c}$	Main rotor 1-per-rev pitch harmonic
$V(t)$	Time dependent control volume
$\mathbf{R}_{i,j,k}$	Flux residuals at cell $(i, j, k)$
$\mathbf{w}_{i,j,k}$	Discretised conserved variables vector
$\rho$	Air density
$\vec{F}_i, \vec{F}_v$	Inviscid and viscous fluxes
$\vec{S}$	Source term

$\vec{w}$	Conserved variables vector
$\vec{\omega}$	Rotor rotational speed
$\vec{u}_h$	Local velocity field in the rotor-fixed FoR

## 1 INTRODUCTION

Thanks to the development of High Performance Computing (HPC) and state-of-the-art Computational Fluid Dynamics (CFD) methods, complete rotorcraft configurations can be simulated with a realistic level of detail and with good accuracy. Validation efforts such as the GOAHEAD project demonstrated the maturity of several modern CFD solvers used for rotorcraft and their usability for a wide range of engineering problems: rotor/fuselage and main/tail rotor interactions, helicopter performances in hover and forward-flight, rotor and airframe design, etc. CFD studies of rotorcraft cover well the entire flight envelope, from hover to high-speed forward flight. In the design phase, it is then possible to estimate the aircraft performance, trim state and attitude that correspond to a particular steady flight condition.

Although hover and steady forward flight account for most of the operating flight time of helicopters, their capabilities are not limited to quasi-steady flight but extend to a variety of manoeuvres: transition from hover to forward flight and aggressive turns, performed in confined areas and turbulent environments such as oil platforms, ship decks, mountain stations, city buildings, etc. Helicopters also exhibit important interactional effects between the rotor wakes and the fuselage,

as well as with their environment. Typical ship wakes shedding frequencies are found to be in the 0.2-2Hz range while pilots consciously respond to frequencies below 1.6Hz [27], the interaction is therefore likely to directly impact the pilot workload during such manoeuvres.

A fully-coupled calculation must take into account these interactions to a certain level of fidelity. Figure 1 presents a simplified description of each element of the global system and the mutual interactions. The yellow frame encompasses the aerodynamic interactional effects, which are implicitly taken into account in the case of a CFD simulation. A helicopter flight mechanics method is required to calculate the aircraft response to the global forces and moments as well as the blades motion. In return, the aircraft response affects simultaneously the aerodynamics of the aircraft and the pilot activity. External disturbances such as wind gusts, sea state, ship motion, etc. are added explicitly to the system.

CFD-based computations are several orders of magnitude slower than a real-time system and cannot be used for on-line simulations. A pilot model needs to be included. The design of control methods and pilot models has been the subject of numerous studies (See Hess [14] for example) and models range from a simple tracking method to complex systems simulating “human-like” responses by including sensory cues, typically physiological and environmental feedback such as visual, vestibular and proprioceptive cues, instruments information, etc.

Moreover, the helicopter can be considered to be in steady or quasi-steady flight only if the contributions of the external disturbances and pilot activity are negligible, i.e. the helicopter can maintain steady flight without any significant change in pilot inputs. If disturbances or pilot activity are added to the system, the helicopter is in manoeuvring flight and it is necessary to model the complete system as presented in the previous paragraph.

### 1.1 Past Work on CFD-based Coupled Methods

Various analytical tools have been developed for the study of rotorcraft dynamics such as HOST [6] and CAMRAD II [16]. They rely on simplified aerodynamic models and are widely used as they provide rapid solutions to a variety of problems. In particular, they include blade aeroelasticity, trimming methods and cover single rotor in hover as well as helicopter in manoeuvring flight. CFD offers extra accuracy but is expensive in terms of CPU time and its use has so far been limited to steady flight conditions.

#### CFD/CSD Coupling

Computational Structural Dynamics (CSD) methods permit to translate the loading on a rotor blade into the corresponding structural deformation. They are usually based on a finite-element method in which the blade is a set of connected beam elements. As noted by Beaumier *et al.* [5], analytical tools are often used prior to a CFD calculation to determine the boundary conditions. However, these methods are limited by the accuracy of the models used. Compressibility, three-dimensional, interactional and viscous effects may not be taken into account and the loads obtained with CFD are potentially more accurate. Coupling the two methods is the only way to achieve consistency between the results.

Beaumier *et al.* [5] and Servera *et al.* [22] from ONERA coupled the Eurocopter comprehensive tool HOST with the CFD code elsA to include blade motion and aeroelasticity into the simulation. Results are compared against experimental data available for the 7A/7AD rotor. Weak “once-per-revolution” and strong “once-per-time-step” coupling methods are investigated. Similar results are found in terms of rotor trim condition and the weak coupling shows to reach convergence more efficiently. However, it is noted that the weak coupling method is appropriate for flight conditions with a periodic solution, i.e. hover or steady forward flight.

A similar method was implemented in the HMB2 solver to couple NASTRAN and HMB [11]. Reference [11] also gives an extensive overview of the literature on CFD/CSD coupling. Results are limited to hover but show reasonable agreement with the experimental data available.

#### Single- and Multi-body Dynamics Coupling

Simulations of the interactional effects between ship and rotorcraft wakes started with the work of Wakefield *et al.* [25] who computed the wake of an actuator disk at different positions over a simplified deck geometry. More recently, Polsky conducted MILES simulations for different scenarios of ship aircraft interaction [19, 20]: V-22 and JSF in hover near the LHA flight deck, static F-14 in front of a jet blast deflector, F-18 following a prescribed landing path above an aircraft carrier deck and a UH60 rotor at different positions above a DDG frigate landing spot. Similarly, actuator discs and source terms were used to model rotors and jet flows but articulated blades and the addition of a flight mechanics model were mentioned as future work.

Despite the high-fidelity of these computations, they are fully prescribed and do not include the aircraft dynamic response. Lee *et al.* [17] studied the ship-helicopter interaction by performing one-way coupled calculations: the ship wake is calculated prior to the calculation and loaded as a set of look-up tables into the analytical tool to simulate the unsteadiness of the ship wake. The method is similar to what is used in most flight-simulation environment and suffers from the use of simplified models in the analytical tool and the lack of feedback from the rotor to the ship wake.

Bridges *et al.* [8] used the same approach but performed two-way calculations in which the information from the rotor loading is fed back to the CFD via the use of source term. Again, the rotor is simulated analytically and the results suffer from several simplifications. However, simulations include the use of a pilot model and the comparison of the results with a human-piloted manoeuvre show similar variations of control history.

### 1.2 Objectives of the Current Work

The objective of the present work is to study the wake interaction encountered during ship/helicopter landing operations by simulating manoeuvring aircraft with CFD. It is a continuation of the work presented earlier [10].

The existing framework of the CFD solver HMB2 developed at the University of Liverpool is used for this work and has been adapted to allow multi-body motion in an earth-fixed frame of reference. A Helicopter Flight Mechanics (HFM) code was developed that solves a multi-body dynamics prob-

lem in a way that is suitable for rotorcraft and can be integrated into HMB2. The coupling is achieved by passing information from HMB to HFM (loads) and HFM to HMB (position and attitude of each element) at each time step of the simulation.

The method is demonstrated using a Sea King helicopter with 5-bladed tail and main rotors and the simplified Canadian Patrol Frigate (CPF). The royal navy typical landing procedure shown figure 2 is chosen as a demonstration case. The aircraft data was made available in a set of manuals of the Australian department of defence [2, 3] and are summarised in table 3. The level of details is considered sufficient for realistic simulations.

A brief description of the CFD solver is presented section 2 along with a description of the typical frame of reference used for the simulation of rotorcraft and the new approach adopted for this work. The multi-body dynamics solver HFM and the coupling with HMB2 are also described. A trimming algorithm and tracking method - based on the linearisation of the aircraft model - have been added to extend the capabilities of HFM. Section 3 presents some elements of validation of the CFD solver for a helicopter at low advance ratio and the prediction of ship wakes. The last section presents the results obtained with the coupled HMB/HFM method for simple test cases. Conclusions are given on the feasibility of the method, the future work is discussed and explore the possibilities offered by the method.

## 2 NUMERICAL METHODS

### 2.1 CFD Solver

The HMB code of Liverpool was used for solving the flow around the different ship and rotor geometries. HMB is a Navier-Stokes solver employing multi-block structured grids. For rotor flows, a typical multi-block topology used in the University of Liverpool is described in Steijl *et al.* [23]. A C-mesh is used around the blade and this is included in a larger H structure which fills up the rest of the computational domain. For parallel computation, blocks are shared amongst processors and communicate using a message-passing paradigm.

HMB solves the Navier-Stokes equations in integral form using the Arbitrary Lagrangian Eulerian (ALE) formulation for time-dependent domains with moving boundaries:

$$\frac{d}{dt} \int_{V(t)} \vec{w} dV + \int_{\partial V(t)} \left( \vec{F}_i(\vec{w}) - \vec{F}_v(\vec{w}) \right) (\vec{n}) dS = \vec{S} \quad (1)$$

where  $V(t)$  is the time dependent control volume,  $\partial V(t)$  its boundary,  $\vec{w}$  is the vector of conserved variables  $[\rho, \rho u, \rho v, \rho w, \rho E]^T$ .  $\vec{F}_i$  and  $\vec{F}_v$  are the inviscid and viscous fluxes, including the effects of the time dependent domain.

The Navier-Stokes equation are discretised using a cell-centred finite volume approach on a multi-block grid, leading to the following equations:

$$\frac{\partial}{\partial t} (\mathbf{w}_{i,j,k} V_{i,j,k}) = -\mathbf{R}_{i,j,k}(\mathbf{w}_{i,j,k}) \quad (2)$$

where  $\mathbf{w}$  represents the cell variables and  $\mathbf{R}$  the residuals.  $i, j$  and  $k$  are the cell indices and  $V_{i,j,k}$  is the cell volume.

Osher's [18] upwind scheme is used to discretise the convective terms and MUSCL variable interpolation is used to provide up to third order accuracy. The Van Albada limiter is used to reduce the oscillations near steep gradients. Temporal integration is performed using an implicit dual-time stepping method. The linearised system is solved using the generalised conjugate gradient method with a block incomplete lower-upper (BILU) pre-conditioner [4].

The HMB2 solver is formulated in the inertial "wind-tunnel" frame of reference. The airframe is fixed and the problem is non-dimensionalised with the farfield velocity. The rotor rotational speed is then adjusted to match the value of the advance ratio. In the case of manoeuvring helicopters, the aircraft is in a non-inertial frame of reference and the advance ratio is not uniquely defined. The previous approach is not valid and it is necessary to choose a new - inertial - frame of reference. The natural "earth-fixed" frame of reference was chosen and the CFD solver was modified accordingly. The differences between the two frames of reference are described in figure 3. The main rotor blade tip velocity in hover was chosen as the new non-dimensional velocity and other variables were scaled accordingly. The definitions of all variables are given in table 1 for each formulation. The table also includes corresponding dimensional values used by the flight-mechanics solver.

### 2.2 Flight Mechanics Method

A Helicopter Flight Mechanics (HFM) method suitable for rotorcraft has been developed and can be used as a standalone code or in a coupled fashion within the CFD framework. The Euler equations of motion for a rigid body are implemented for the helicopter fuselage and each rotor blade. The global set of differential equations is solved using the Euler or RK4 method. A trimming sequence is added at the beginning of the calculation to determine the appropriate trim state. The trimming method is described in more detail section 2.3.

The standalone version uses simplified models for the aircraft aerodynamics and therefore a number of approximations are made. The use of CFD permits to alleviate some of these approximations. A comparison of the level of approximation of each method is given table 2.

### 2.3 Trimming Method

A simple linearisation method was implemented that permits to calculate a jacobian matrix from any set of variables and parameters:

$$J = \left( \frac{\partial F_i}{\partial x_j} \right)_{i,j} \quad (3)$$

$F_i$  is the value of the variable  $f_i$  integrated over a representative time, typically  $\Delta t = \frac{2\pi}{\omega N_{blades}}$ , i.e. one period of the rotor loads, to take into account only the mean value of the variable:

$$F_i = \int_{\Delta t} f_i(t) dt \quad (4)$$

Partial derivatives are calculated using centered finite differences:

$$J_{i,j} = \frac{F_i(x_j + \epsilon) - F_i(x_j - \epsilon)}{2\epsilon} \quad (5)$$

$$y = Cx \quad (12)$$

Trimming the helicopter rotor consists in finding the appropriate pilot inputs and aircraft attitude to keep the aircraft in a predetermined steady flight. The method constructs a jacobian matrix (equation 3) from a chosen set of parameters (equation 6) and variables (equation 7) and uses this matrix to find the values of the pilot inputs that minimise the budget of forces and moments applied to the body in the 6 directions. The 4 pilot inputs and 2 body attitude angles are chosen as parameters so as to obtain a 6 equations/6 variables system.

$$x = (\theta_0^M \theta_{1c} \theta_{1s} \theta \Phi \theta_0^T)^T \quad (6)$$

$$f = (F_x F_y F_z L M N)^T \quad (7)$$

The problem then consists in calculating the update value for the parameters  $\tilde{x}$  so that the loads  $\tilde{f}$  tend toward zero:

$$\tilde{x}_n = J_n^{-1} \tilde{f}_n \quad (8)$$

The matrix  $J_n$  is recalculated before each iteration  $n = [1 \dots N]$  of the trimmer to obtain the local derivatives and increase stability and convergence speed.

## 2.4 Manoeuvring Flight

The trimming method is suitable for determining the controls to apply to the aircraft to maintain hover or steady flight. More advanced methods use the CFD loads directly, usually in a loosely coupled fashion [12].

However, during a manoeuvre, the aircraft is out-of-trim and the global loads applied to the system are not null. In case of manoeuvre, the pilot controls must then be in accordance with the objective of the manoeuvre, typically following a predetermined flight path, hence requiring a strong coupling between the loads and the changes in control inputs.

To simulate manoeuvring helicopters, control methods were developed and designed for optimal tracking or to be representative of the behavior of a real pilot. The SYCOS method has been widely used in the past [7, 24] and is based on inverse simulation: a linear system is written (equation 9) where  $A$  and  $B$  are two jacobian matrices that correspond to the aircraft response to changes in attitude and pilot controls respectively. The inverse system (equation 14) then provides a way to estimate the pilot controls corresponding to a pre-determined flight path.

A typical formulation for inverse modeling is the following:

$$\dot{x} = Ax + Bu \quad (9)$$

Where:

$$x = (u v w p q r \phi \theta \Psi)^T \quad (10)$$

$$u = (\theta_0^M \theta_{1c} \theta_{1s} \theta_0^T)^T \quad (11)$$

$x$  and  $u$  are the state and control vectors respectively. An output equation is necessary to select the prescribed variables:

$y$  contains only the values of the prescribed variables, typically the earth-based components of velocity and the heading angle, so that :

$$y = (u_e v_e w_e \Psi)^T \quad (13)$$

Pilot controls come directly from the inverse problem:

$$u^* = (CB)^{-1}(y^* - CAx) \quad (14)$$

Where  $y^*$  is the prescribed trajectory and  $u^*$  the variation of the pilot inputs around the trim state. By prescribing  $y^*$ , the inverse modeling method gives a prediction of the pilot controls required to follow exactly the trajectory. A short reposition manoeuvre was designed to represent the second branch of a standard ship landing procedure. The Linear-Quadratic Regulator (LQR) method was used to simulate a piloted flight. The method updates the pilot controls in order to minimise the error in position and attitude using a least-square minimisation algorithm. Figure 12 compares the pilot inputs predicted using inverse modeling with the results of a piloted simulation that uses the LQR method.

The  $A$  and  $B$  matrices can be determined analytically only in a few simple cases and the linearisation method presented in the previous section is used for this work. The SYCOS method uses an approximate linear inverse model along with a correction method to build a simple tracking method that can be used as a simple pilot model to follow a pre-determined flight path. This very simple model has several limitations: the linear model is valid only around the trimmed condition, which is used to initiate the manoeuvre. Manoeuvres also need to be smooth (typically  $C^2$  continuous) and not overly aggressive to avoid oscillations that lead to unrealistic results.

The SYCOS method proved to be suitable for simulating standard manoeuvres described in the ADS33 documentation such as the slalom [24].

## 3 VALIDATION WORK

The objective of simulating ship/helicopter landing manoeuvres requires to validate the CFD code HMB2 for helicopter configurations at low advance ratio as well as ship wakes and demonstrate the feasibility of simultaneous computations.

### 3.1 Ship Airwake Validation

The sharp edges typical of most ship geometries are known to fix the points of separation in the flow and generate large zones of recirculation in the vicinity of the superstructure. The wake is typically unsteady, with shedding frequencies in the range 0.2-2Hz depending on the size of the elements of the superstructure and the wind speed. The Reynolds number based on the ship length is typically around 100 millions for a frigate while the Mach number is below 0.1.

The Simple Frigate Shape (SFS2) was designed for validation purposes and experimental data from NRC in Canada [9, 26] and the Naval Surface Warfare Center Carderock Division (NSWCCD) [21] have been published.

Figure 6(a) shows the positions of the probes used in the NSWCCD experiments. The mean values of streamwise velocity as well as local flow pitch and yaw angle are available.

Detached Eddy Simulation coupled with the Spalart-Allmaras turbulence model was used for the CFD simulations. A grid density study, Figure 5 showed that a fine grid containing 15 million cells was required to capture the unsteadiness of the flow. A dominant shedding frequency of about 0.6Hz is found which is within the 0.2-2Hz range typical of ship air-wakes.

Results in terms of streamwise velocity and local pitch and yaw angles are presented in Figure 6 for the 60 degrees side wind case. Agreement between experimental and CFD data is reasonable with some discrepancies found close to the deck and around the centreline of the ship where the deficit of velocity is over-predicted by the CFD.

### 3.2 Helicopter Configuration Validation

The low-speed case "TC2" of the GOAHEAD database is used to validate HMB2 for helicopter configurations at low advance ratio [1]. The advance ratio is close to 0.1 and the aircraft has a nose-up pitch angle of 1.9 degrees. The main rotor pitch and flap harmonics were predicted using HOST and the same values are used here, without retrimming. This case is characterized by important blade/vortex and vortex/tail interactions due to the low advance ratio.

The experimental data available includes recordings of unsteady pressure on the fuselage, fin, tail and main rotor blades, as well as PIV measurements in the region above the tail plane.

Figure 8 shows distribution of mean pressure coefficient for 3 fuselage sections and good agreement with the experimental data is found in all regions of the body. Three probes were chosen to show the unsteady pressure signals at key locations on the body: below the rotor, on the side of the fuselage and on the side of the fin. Clear 4-per-rev and 10-per-rev peaks in the signals are found that correspond to the main and tail rotor blade passing frequencies. The peak-to-peak values are accurately predicted in most locations, giving confidence in the global load prediction, including the unsteady characteristics.

Pressure levels on the main rotor, figure 10 show reasonable agreement, although they suffer from the uncertainty on the rotor trim values. Agreement is good around the azimuth but inboard loads are better predicted overall.

## 4 DEMONSTRATION OF THE METHOD

### 4.1 Ship/Helicopter Interaction Simulation

The CFD solver HMB2 has demonstrated good capabilities for the predicting of ship airwakes and helicopter aerodynamics at low advance ratio independently. Coupled calculations with an aircraft moving with respect to the ship requires the use of the chimera method that has already been implemented [15]. Two static simulations were run to demonstrate the capabilities of the solver: helicopter centered above the deck and on the side of the ship, in hover, that correspond to

typical near-hover positions achieved during the landing manoeuvre. Figure 11 shows the pressure coefficients on the ship and helicopter bodies for each simulation and the wake visualisation shows signs of ship/rotor wake interference already suggested in a previous paper [10] using simpler methods.

An extended grid-motion method was also implemented that combines relative motion between the different elements of the simulation and a grid deformation method that allows the rotor blades to rotate in pitch, flap and lead-lag.

The helicopter-fixed frame of reference typically used for forward flying rotors is not appropriate for manoeuvring helicopters and an earth-fixed frame of reference was used instead. The normalisation of the computation variables is done using the main rotor tip speed in hover as reference. The differences in formulation of the solver between the "normal" and "manoeuvre" modes are summarised in table 1.

### 4.2 Coupled HFM/HMB Simulations

The Helicopter Flight Mechanics solver has been integrated into the HMB2 environment and integrates the trimming, inverse modeling and LQR pilot functions. A typical coupled calculations follows multiple steps: initial trimming using simplified models, calculation of the linear model for the LQR pilot method, CFD calculation of the manoeuvre using inverse modeling or LQR tracking method to adjust the pilot controls. Figure 12(a) shows the aircraft position and attitude predicted using inverse modeling and obtained using the LQR tracking method, throughout the manoeuvre. LQR pilot model follows the prescribed trajectory accurately, with a small overshoot and overall lag in response compared to the inverse-modeling prediction. The control angles (Figure 12(b)) predicted using inverse-modeling show variations around the trim condition, where all values are zero, while the LQR results are actual values. The main and tail rotor collective angles show similar results, with little changes in main rotor collective due to the low speed of the manoeuvre but high changes in tail rotor collective due to the reduced inflow from the lateral velocity. The main rotor cyclic angles show similar trends but larger variations are found for the LQR results. The overall lag observed on the position and attitude is seen on the control angles as well.

Figure 13 shows the loads on the fuselage, main rotor and tail rotor obtained using the simplified models in HFM and the CFD for trimmed forward flight case. The aircraft was trimmed using HFM prior to the calculation. Results show clearly the influence of the main and tail rotor blades on the fuselage loads and the global CFD loads of the main and tail rotors are in good agreement with the values predicted using HFM.

## 5 CONCLUSIONS AND FUTURE WORK

CFD provides accurate tools for predicting both ship and rotorcraft wakes and the development of High Performance Computing and CFD methods now permit such simulations.

The CFD code HMB2 was first validated for ship wake prediction using the experimental data gathered on the Simple Frigate Shape. The results obtained showed good agreement in terms of mean flow topology. Moreover, a grid den-

sity study showed that adequate levels of unsteadiness in the vicinity of the deck require the use of a DES model on a 15 million cells grid. Further validation was carried out for full rotorcraft configurations at low advance ratio using the GOA-HEAD experimental data. Results in terms of loads on the fuselage were good in terms of mean and time-dependent values. The loads on the blades were also well predicted despite some uncertainty on the exact trim state.

A Flight Mechanics solver and a pilot model have been coupled to the CFD environment HMB2 and the objectives were two-fold: designing a full helicopter trimmer based on CFD loads, and simulate manoeuvring aircraft. The simulation of manoeuvring aircraft requires the adoption of a new “earth-fixed” frame of reference as well as a more versatile grid motion approach. These were implemented in HMB2 and validated. A chimera method will be used for coupled calculations and have been demonstrated by performing three unsteady “station-keeping” simulations of the aircraft at three positions along the typical landing path. Results show the expected interference between the ship and helicopter wake that occurs when the helicopter is in the direct vicinity of the ship.

A short lateral reposition manoeuvre was chosen to be representative of the second branch of a typical ship landing manoeuvre and was chosen for development purposes. The integration of the flight mechanics and LQR pilot methods into the CFD environment were demonstrated via a dummy simulation and a fixed hover simulation showed similar loads. Future simulations will substitute the approximate models for the loads obtained with CFD, but present results give confidence in the method.

## 6 ACKNOWLEDGEMENTS

The support of this project by AgustaWestland Liverpool Advanced Rotorcraft Center is gratefully acknowledged. The authors would like to thank the N8 High Performance Computing (N8 HPC) centre for the use of CPU time.

## REFERENCES

- [1] A.F. Antoniadis, D. Drikakis, B. Zhong, G. Barakos, R. Steijl, M. Biava, L. Vigevano, A. Brocklehurst, O. Boelens, M. Dietz, M. Embacher, and W. Khier. Assessment of CFD Methods Against Experimental Flow Measurements for Helicopter Flows. *Aerospace Science and Technology*, 19(1):86–100, 2012. GOAHEAD.
- [2] AM Arney and NE Gilbert. A user’s manual for the arl mathematical model of the sea king mk-50 helicopter: Part 1. basic use. Technical report, DTIC Document, 1988.
- [3] AM Arney and NE Gilbert. A user’s manual for the arl mathematical model of the sea king mk-50 helicopter: Part 2. use with arl flight data. Technical report, DTIC Document, 1988.
- [4] O. Axelsson. *Iterative Solution Methods*. Cambridge University Press: Cambridge, MA, 1994.
- [5] P Beaumier, M Costes, O Rodriguez, M Poinot, and B Cantaloube. Weak and strong coupling between the elsolver and the host helicopter comprehensive analysis. *ONERA: Tire a Part*, (186):1, 2005.
- [6] Bernard Benoit, K Kampa, W von Grunhagen, P-M Basset, and B Gimonet. Host, a general helicopter simulation tool for germany and france. In *Annual Forum Proceedings of the American Helicopter Society*, volume 56, pages 1110–1131, 2000.
- [7] R. Bradley and G. Brindley. Progress in the Development of a Versatile Pilot Model for the Evaluation of Rotorcraft Performance, Control Strategy and Pilot Workload. *Aeronautical Journal*, 107(1078):731–738, 2003.
- [8] D. O. Bridges, J. F. Horn, E. Alpman, and L. N. Long. Coupled flight dynamics and cfd analysis of pilot workload in ship airwakes. In *Collection of Technical Papers - 2007 AIAA Atmospheric Flight Mechanics Conference*, volume 1, pages 471–489, 2007.
- [9] B.T. Cheney and S.J. Zan. CFD Code Validation Data and Flow Topology for TCCP AER-TP-2 Simple Frigate Shape. *Ottawa, Canada*, 1999.
- [10] C. Crozon, R. Steijl, and G.N. Barakos. Numerical Study of Rotor in Ship Airwake. *39th European Rotorcraft Forum 2013, ERF 2013*, 2013.
- [11] F. Dehaeze and G.N. Barakos. Hovering Rotor Computations Using an Aeroelastic Blade Model. *Royal Aeronautical Society*, 116(1180), 2012.
- [12] M.a Embacher, M.a KeÅ§ler, M.b Dietz, and E.a KrÃd’mer. Capability of helicopter cfd-simulation trimmed to free flight condition to predict flight test data. pages 1058–1069, 2011.
- [13] RA Feik and RH Perrin. Identification of an Adequate Model for Collective Response Dynamics of a Sea King Helicopter in Hover. Technical report, DTIC Document, 1988.
- [14] R.A. Hess. Simplified technique for modeling piloted rotorcraft operations near ships. *Journal of guidance, control, and dynamics*, 29(6):1339–1349, 2006.
- [15] M. Jarkowski, M.A. Woodgate, G.N. Barakos, and J. Rokicki. Towards Consistent Hybrid Overset Mesh Methods For Rotorcraft CFD. *International Journal for Numerical Methods in Fluids*, 2011.
- [16] Wayne Johnson. Technology Drivers in the Development of CAMRAD II. In *American Helicopter Society Aeromechanics Specialists Conference, San Francisco, California*, 1994.
- [17] D. Lee and J.F. Horn. Simulation of pilot workload for a helicopter operating in a turbulent ship airwake. *Proceedings of the Institution of Mechanical Engineers, Part G: Journal of Aerospace Engineering*, 219(5):445–458, 2005.
- [18] S. Osher and S. Chakravarthy. Upwind Schemes and Boundary Conditions with Applications to Euler Equations in General Geometries. *Journal of Computational Physics*, 50:447–481, January–February 1983.

- [19] S. Polsky. Progress Towards Modeling Ship/Aircraft Dynamic Interface. In *HPCMP Users Group Conference, 2006*, pages 163–168. IEEE, 2006.
- [20] S.A. Polsky. Computational Analysis for Air/Ship Integration: 1st Year Report. In *High Performance Computing Modernization Program Users Group Conference (HPCMP-UGC), 2010 DoD*, pages 109–114. IEEE, 2010.
- [21] E. W. Quon, P. A. Cross, Smith M. J., Rosenfeld N. C., and Whitehouse G. R. Investigation of Ship Airwakes Using a Hybrid Computational Methodology. In *AHS 70th Annual Forum, Montreal, Quebec*, 2014.
- [22] Gaelle Servera, Philippe Beaumier, and Michel Costes. A weak coupling method between the dynamics code host and the 3d unsteady euler code waves. *Aerospace science and technology*, 5(6):397–408, 2001.
- [23] R. Steijl, G. Barakos, and K. Badcock. A Framework for CFD Analysis of Helicopter Rotors in Hover and Forward Flight. *International Journal for Numerical Methods in Fluids*, 51(8):819–847, 2006.
- [24] Douglas Thomson and Roy Bradley. Inverse simulation as a tool for flight dynamics research - principles and applications. *Progress in Aerospace Sciences*, 42(3):174 – 210, 2006.
- [25] NH Wakefield, SJ Newman, and PA Wilson. CFD Predictions of the Influence of External Airflow on Helicopter Operations When Operating From Ship Flight Decks. In *RTO applied vehicle technology panel symposium*, pages 2–1, 1999.
- [26] S.J. Zan. Surface Flow Topology for a Simple Frigate Shape. *Canadian Aeronautics and Space Journal*, 47(1):33–43, 2001.
- [27] S.J. Zan. On Aerodynamic Modeling and Simulation of the Dynamic Interface. *Proceedings of the Institution of Mechanical Engineers, Part G: Journal of Aerospace Engineering*, 219(5):393–410, 2005.

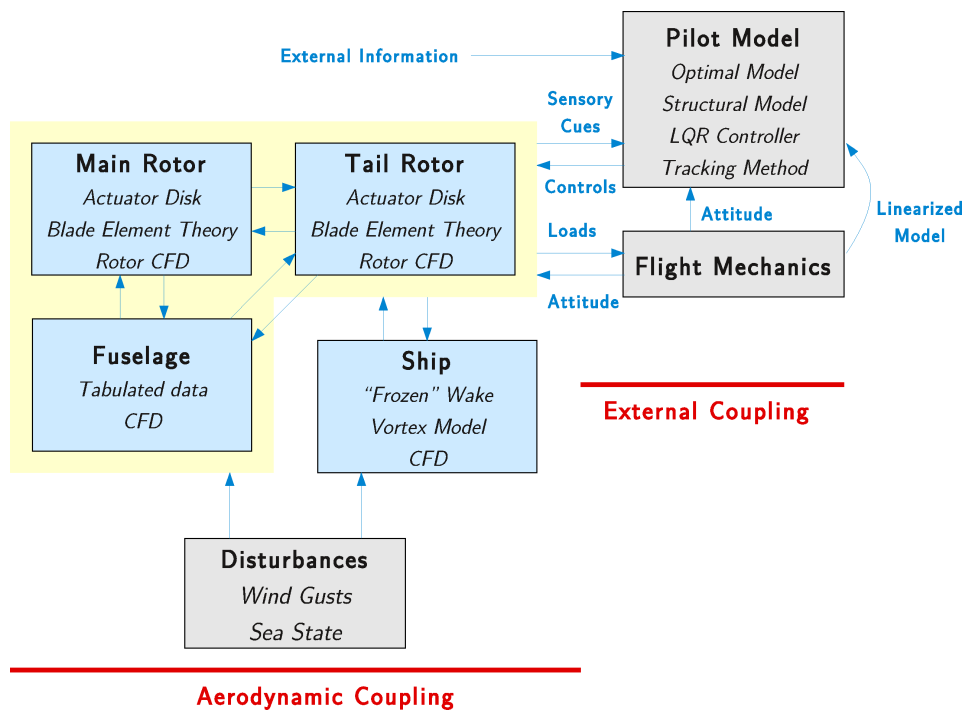


Figure 1: Description of the couplings associated with the simulation of the Dynamic Interface.

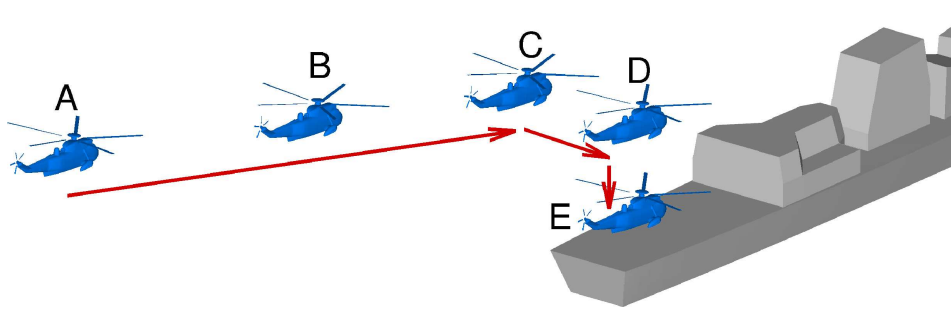
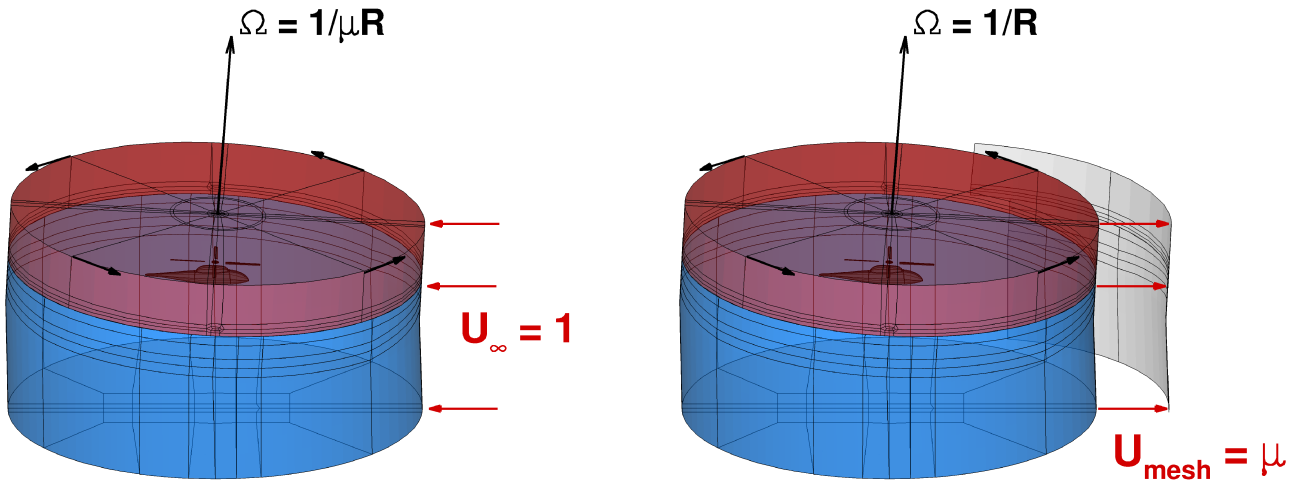


Figure 2: Typical landing procedure. A,B) Forward flight along the ship, C) stabilisation of the aircraft, D) Lateral translation and hover, E) Landing.



(a) Wind-tunnel frame of reference

(b) Earth-fixed frame of reference

Figure 3: Wind-tunnel frame of reference is the classic approach of helicopter CFD. An earth-fixed frame of reference is used for the simulation of freely-flying aircraft.

Non-dimensional variable	Baseline HMB	HMB in vehicle mode	Helicopter Flight Mechanics
Tip velocity $V_{tip}$	$V_{tip} = \frac{1}{\mu}$	$V_{tip} = 1$	$V_{tip} = \omega R$
Rotational velocity	$\omega = \frac{1}{\mu R}$	$\omega = \frac{1}{R} (V_{tip} = 1)$	$\omega = \frac{V_{tip}}{R}$
Time step	$\Delta t = \frac{2\pi\mu R}{N_{steps/cycle}}$	$\Delta t = \frac{2\pi R}{N_{steps/cycle}}$	$\Delta t = \frac{2\pi R}{N_{steps/cycle} V_{tip}}$
Reference length	1 rotor chord length	1 meter	1 meter
Azimuthal step $\omega \Delta t$	$\Delta \Psi^{main} = \frac{360}{N_{steps/cycle}}$	$\Delta \Psi^{main} = \frac{360}{N_{steps/cycle}}$	$\Delta \Psi^{main} = \frac{360}{N_{steps/cycle}}$

Table 1: Definitions and correspondences between HFM and HMB codes. As of now  $V_{tip}$  is more or less arbitrary, the user should make sure it is consistent with the provided Mach number.

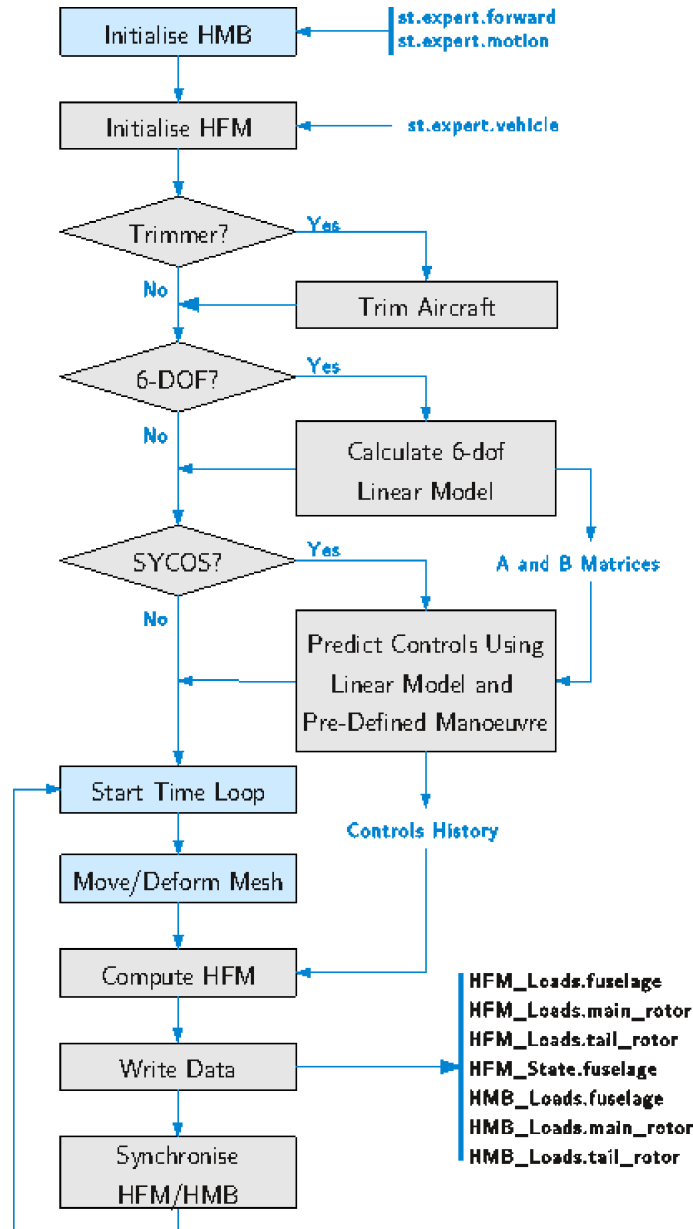
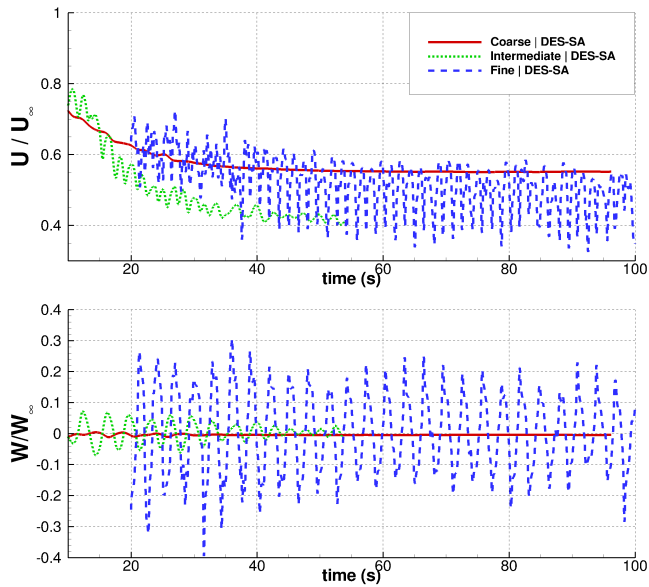


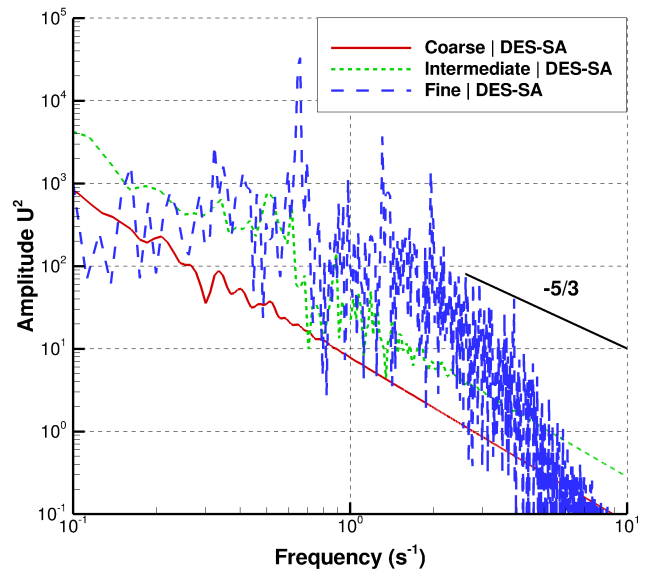
Figure 4: Implementation of the standalone Flight Mechanics code.

Parameter	Standalone Flight Mechanics model	Coupled HFM/CFD
6DOF fuselage	✓	✓
Articulated blades	✓	✓
Atmospheric conditions	✓	✓
Inflow	✓(Linear model)	✓
Control surfaces	✓(bi-linear model)	✓
Blade aerodynamics	✓(Blade Element Theory)	✓
Rotor/fuselage interaction	✗	✓
Blade-tip losses	✗	✓
3D effects	✗	✓
Flexible blades	✗	✗

Table 2: Comparison between standalone flight mechanics and CFD coupling approximations.

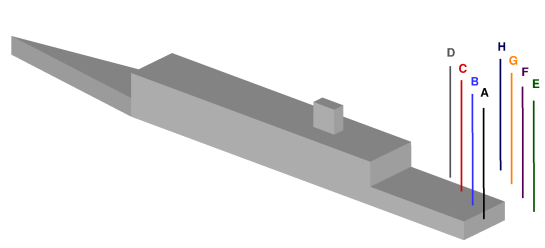


(a) Velocity history



(b) Frequency analysis

Figure 5: Grid density study using DES-SA model on the Simple Frigate Shape. A fine grid is required to capture the flow unsteady characteristics and the typical shedding frequency is around 0.5Hz.  $WOD = 0$  degrees,  $Re = 6.5810^5$



(a) 60 degrees Sidewind

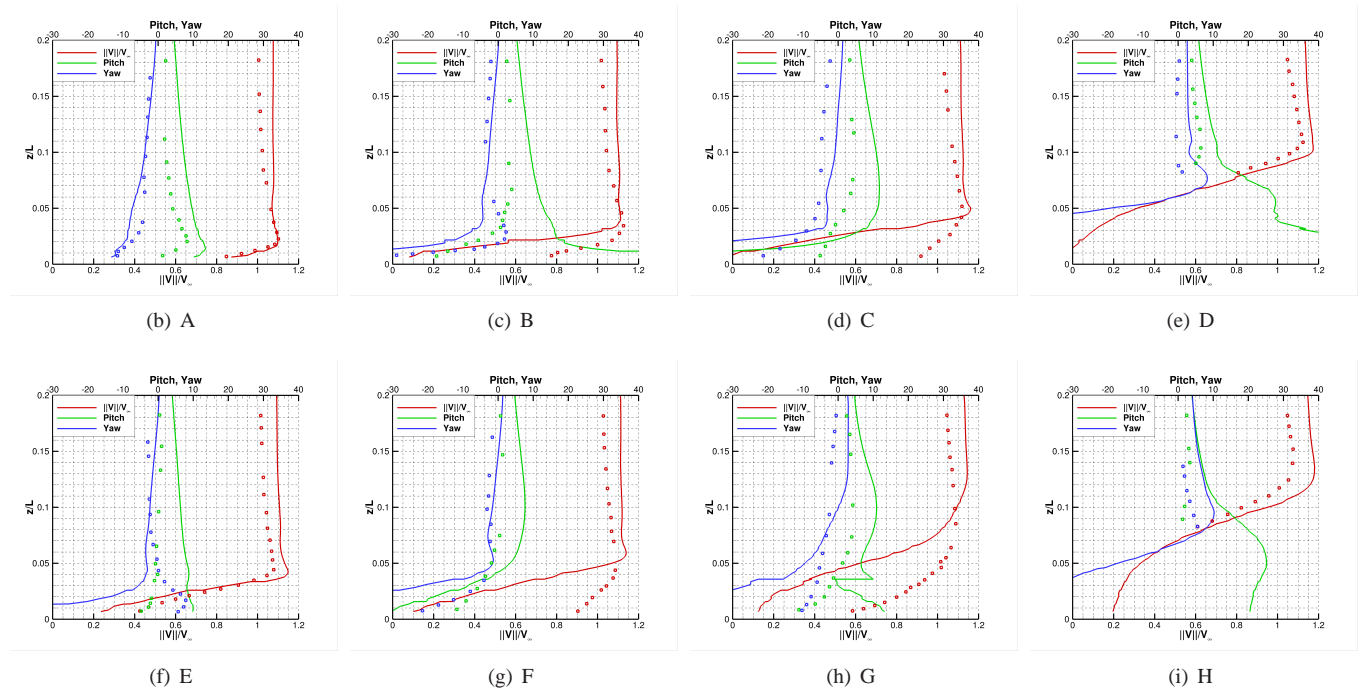
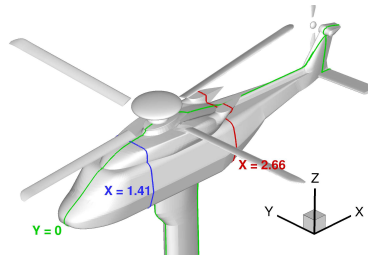
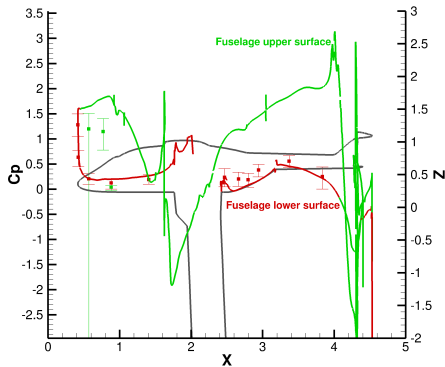


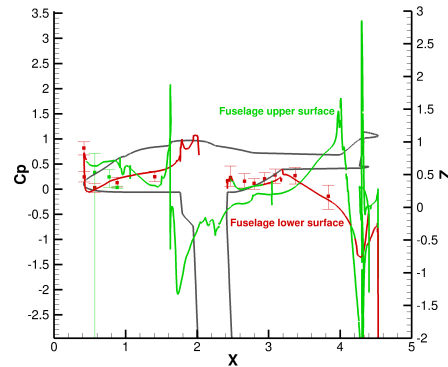
Figure 6: Mean values of velocity and flow angles along 8 vertical lines.  $WOD = 60$  degrees,  $Re = 6.5810^5$



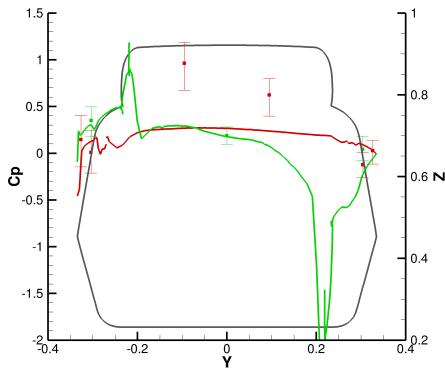
(a) Positions of slices



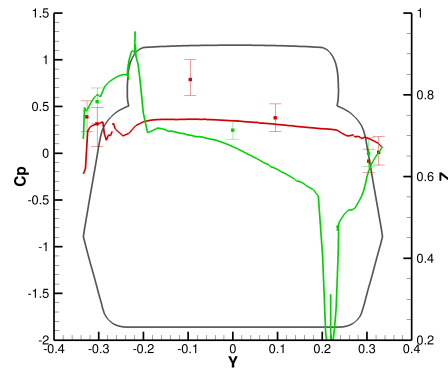
(b) Slice Y=0 - 0 degrees



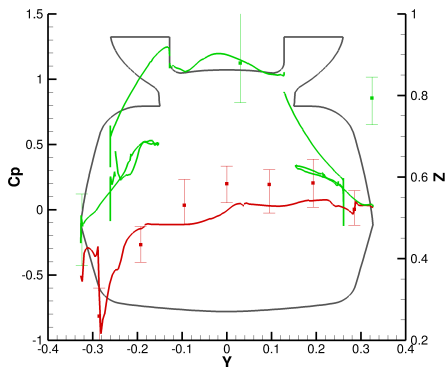
(c) Slice Y=0 - 45 degrees



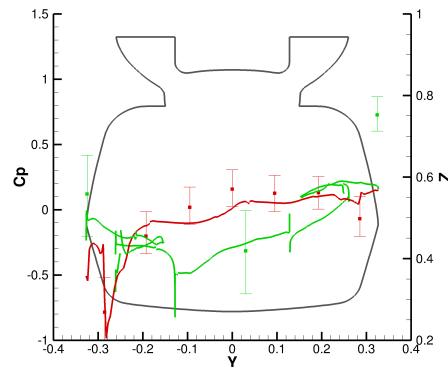
(d) Slice X=1.41 - 0 degrees



(e) Slice X=1.41 - 45 degrees

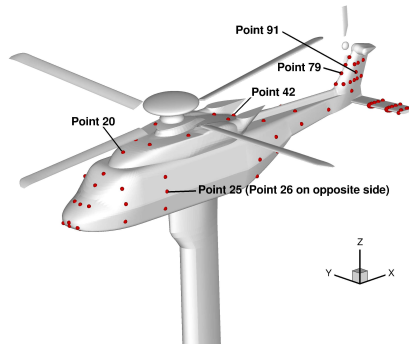


(f) Slice X=2.66 - 0 degrees

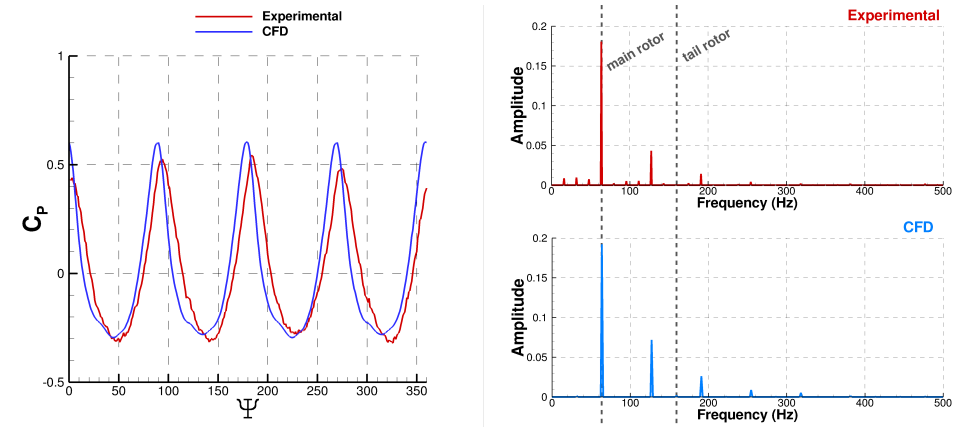


(g) Slice X=2.66 - 45 degrees

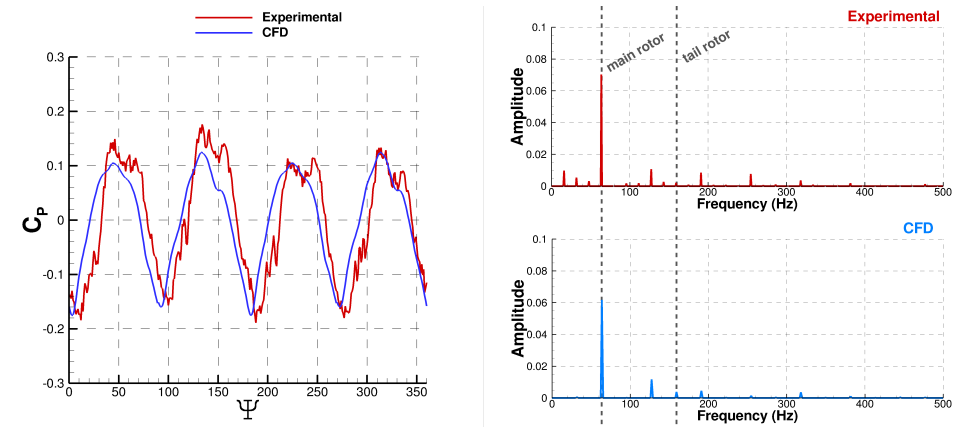
Figure 7: Distribution of pressure coefficient for three sections of the fuselage at 0 and 45 degrees blade azimuth.



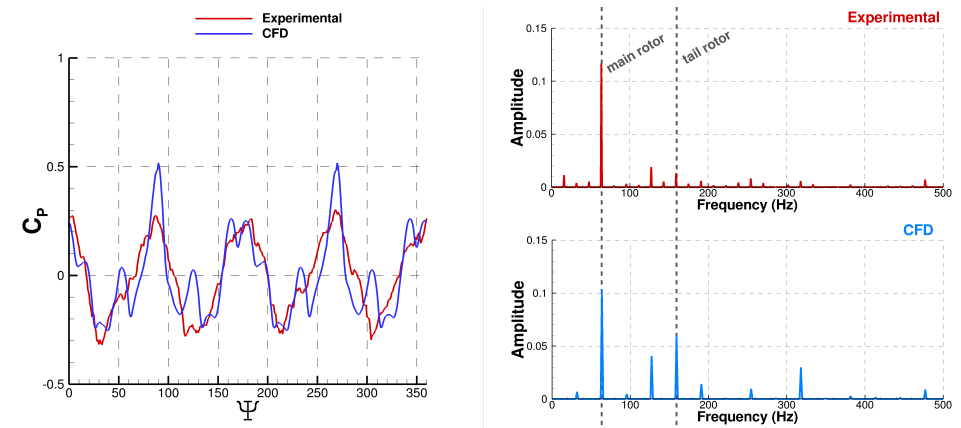
(a) Positions of probes



(b) Point 20

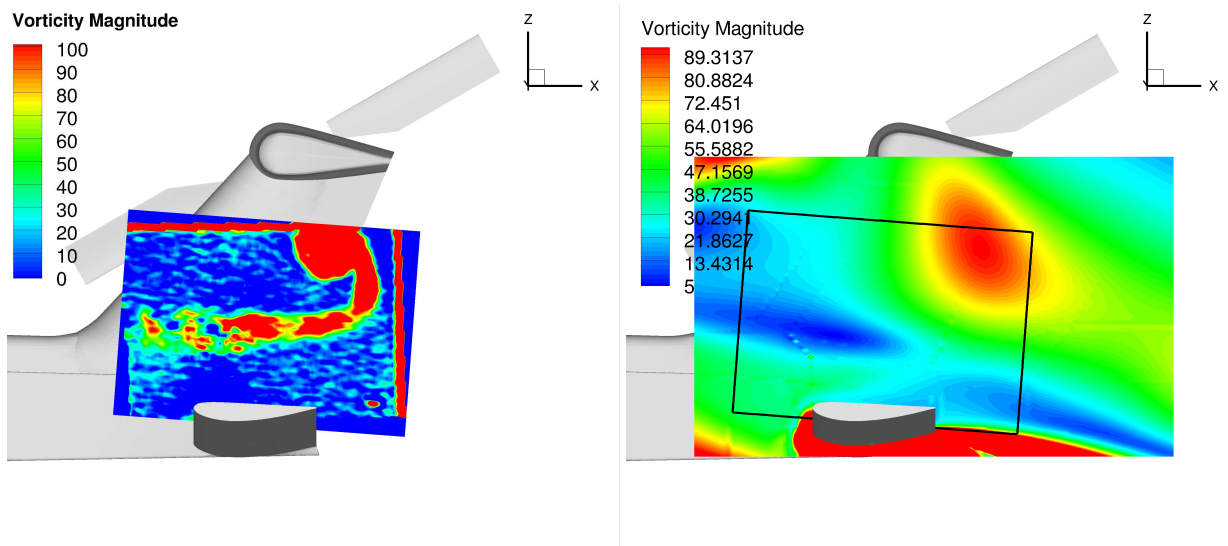


(c) Point 25

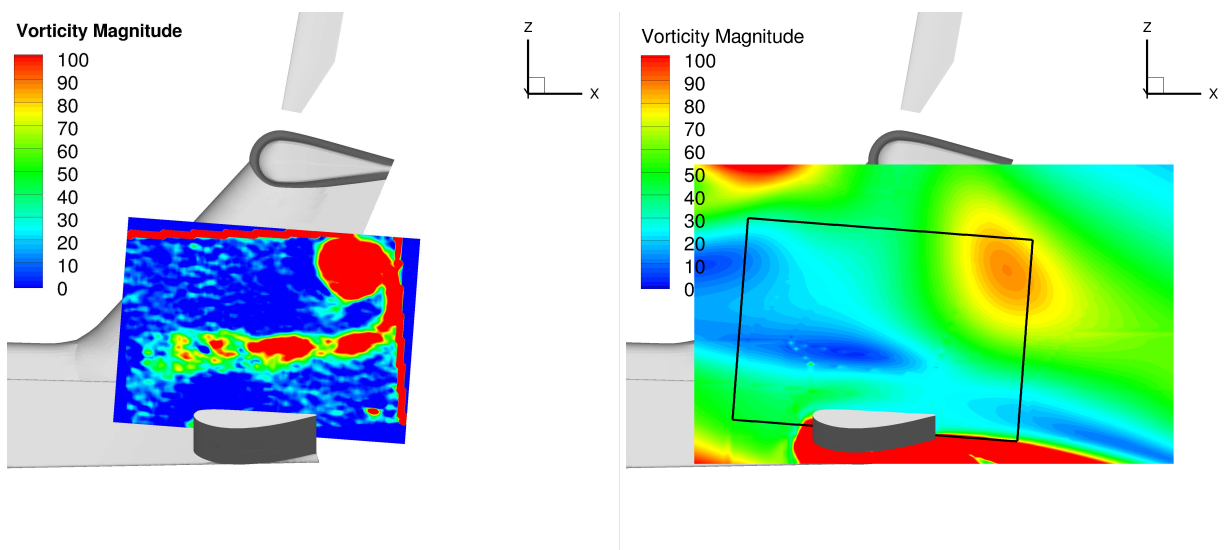


(d) Point 91

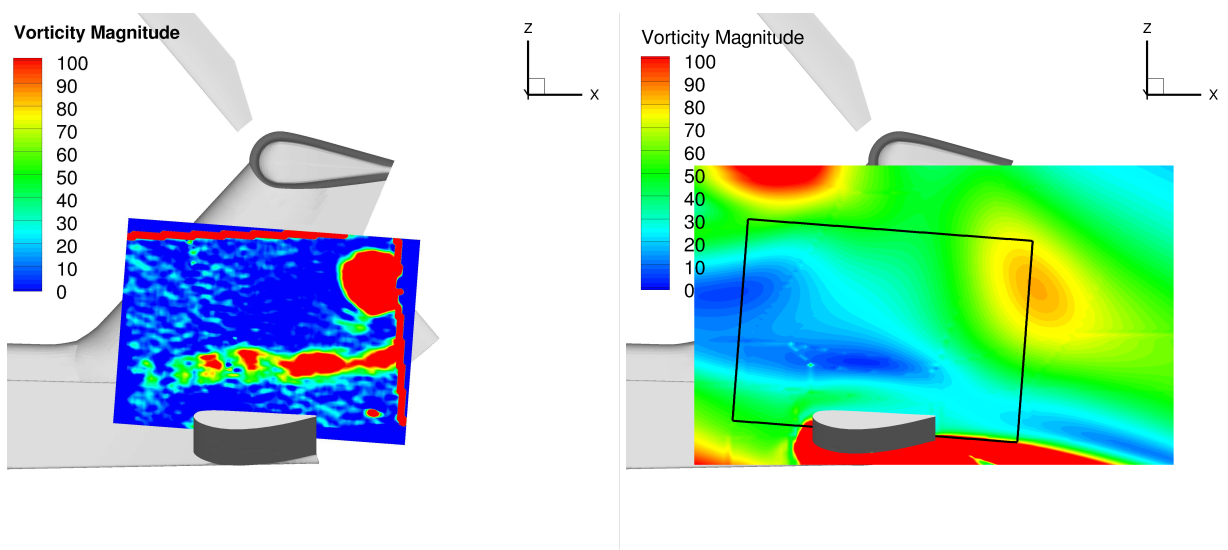
Figure 8: Signal of pressure as function of blade azimuth (mean removed) and FFT decomposition of the signal for 3 different points on the fuselage.



(a) 60 degrees

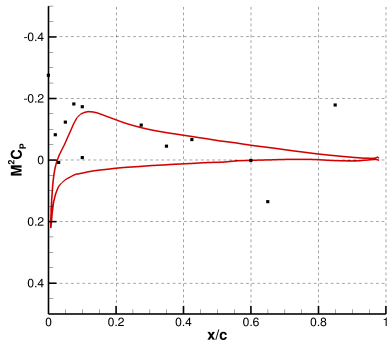


(b) 70 degrees

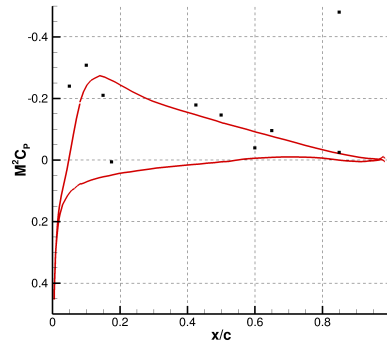


(c) 80 degrees

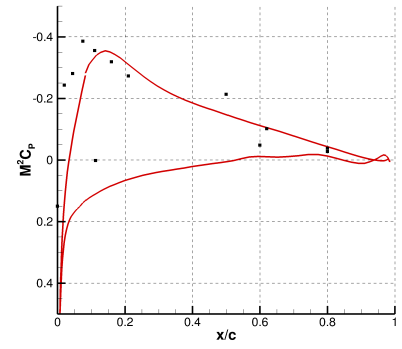
Figure 9: Comparison of the PIV data (left) and numerical results (right) for the flowfield over the tail plane for 3 different azimuth of the main rotor.



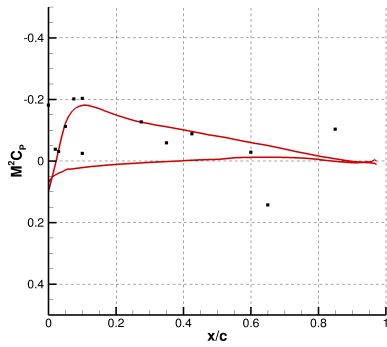
(a)  $\Psi = 0$  degrees,  $r/R = 50\%$



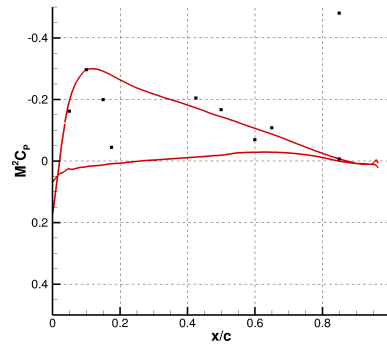
(b)  $\Psi = 0$  degrees,  $r/R = 70\%$



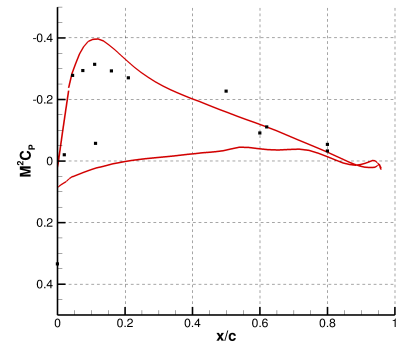
(c)  $\Psi = 0$  degrees,  $r/R = 82.5\%$



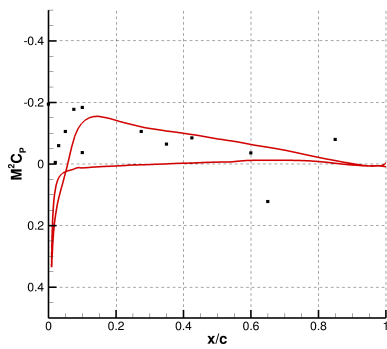
(d)  $\Psi = 60$  degrees,  $r/R = 50\%$



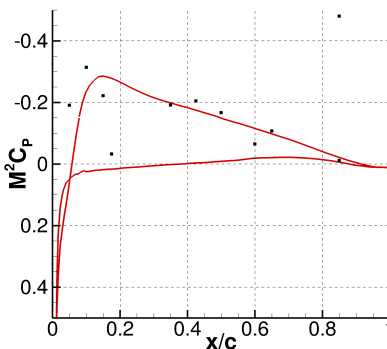
(e)  $\Psi = 60$  degrees,  $r/R = 70\%$



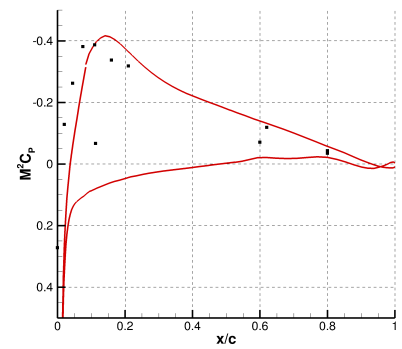
(f)  $\Psi = 60$  degrees,  $r/R = 82.5\%$



(g)  $\Psi = 120$  degrees,  $r/R = 50\%$



(h)  $\Psi = 120$  degrees,  $r/R = 70\%$



(i)  $\Psi = 120$  degrees,  $r/R = 82.5\%$

Figure 10: Curves of experimental and numerical pressure coefficient at 0 and 60 degrees for 3 different spanwise locations: 50%, 70% and 82.5%.

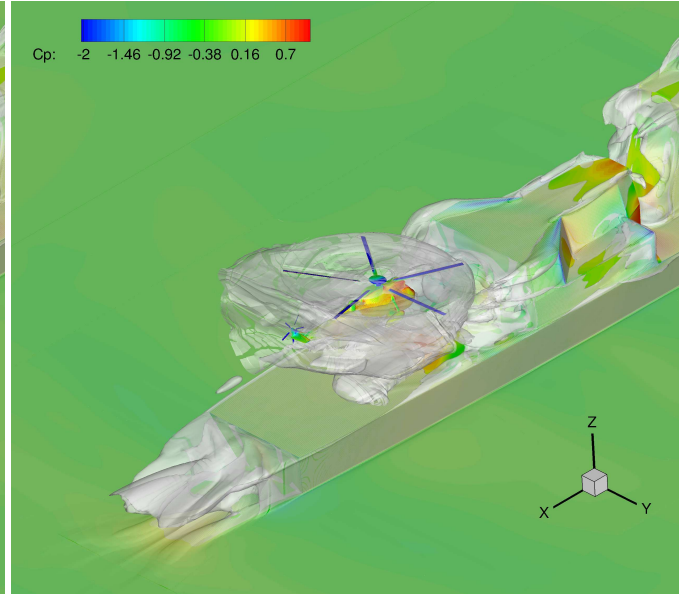
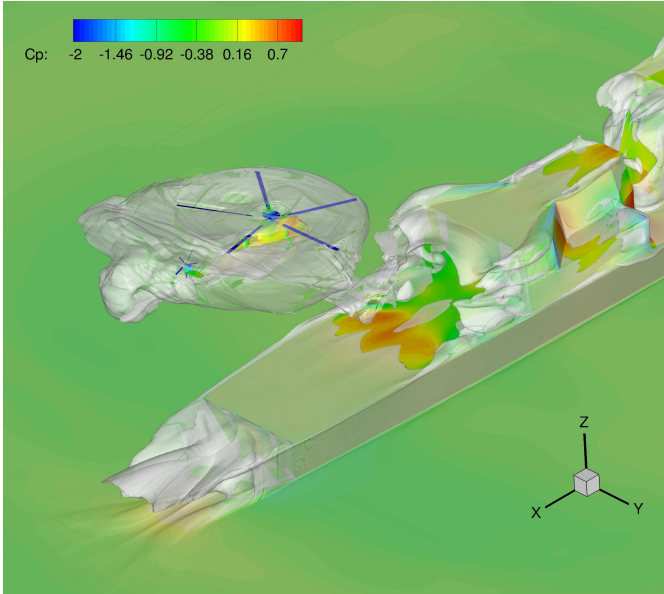
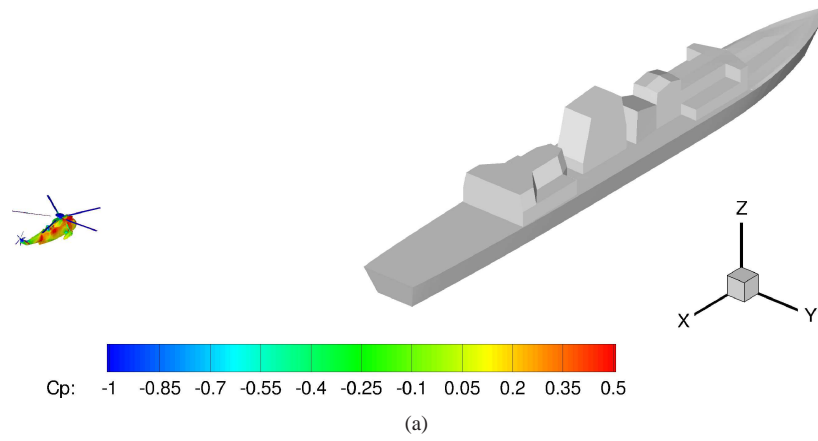
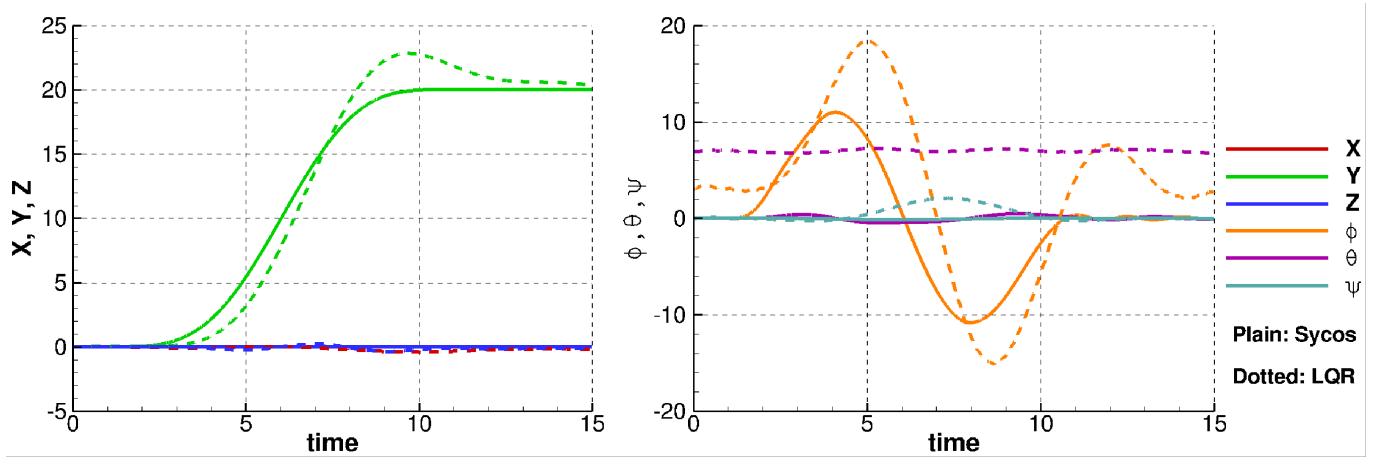


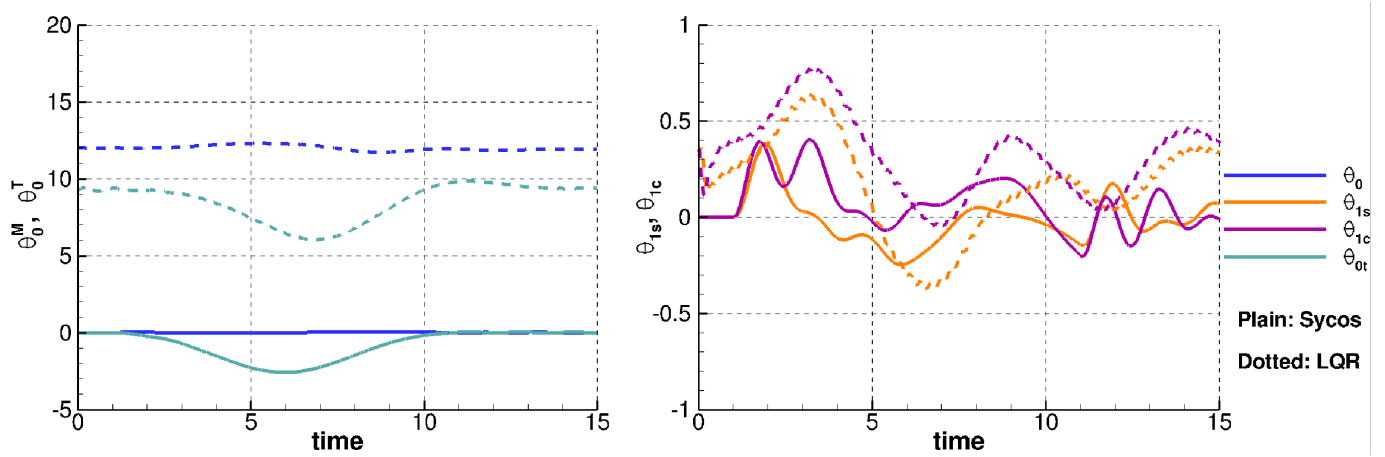
Figure 11: Station-keeping Sea King at three different positions: (a) Forward-flight, (b) hover on the side of the deck, (c) hover above the deck before touchdown.

Variable	DTIC Value	SI value
All Up Weight (AUW)	18500 <i>lb</i>	8391.46 <i>kg</i>
Main rotor lock number	10.76	10.76
Tail rotor lock number	5.10	5.10
Roll 2nd moment of inertia	14275 <i>slugs.ft<sup>2</sup></i>	19354.3 <i>kg.m<sup>2</sup></i>
Pitch 2nd moment of inertia	48375 <i>slugs.ft<sup>2</sup></i>	65587.69 <i>kg.m<sup>2</sup></i>
Yaw 2nd moment of inertia	39150 <i>slugs.ft<sup>2</sup></i>	53080.27 <i>kg.m<sup>2</sup></i>
CGz*	145 <i>inches</i>	3.683 <i>m</i>
CGx*	-1.03 <i>inches</i>	-0.026 <i>m</i>
Rotor radius	31 <i>ft</i>	9.4488 <i>m</i>
Blade chord	1.52 <i>ft</i>	0.4633 <i>m</i>
Hinge offset	1.05 <i>ft</i>	0.32 <i>m</i>
Blade twist	-8.0 <i>degrees</i>	-8.0 <i>degrees</i>
Blade mass	181 <i>lb</i>	82.1 <i>kg</i>
Rotation speed $\Omega$	21.89 <i>rd.s<sup>-1</sup></i>	21.89 <i>rd.s<sup>-1</sup></i>
Lock Number $\gamma$	11.51	11.51
Ratio rotor/blade inertia	6	6
Main rotor forward angle (from 3)	4.2 <i>degrees</i>	4.2 <i>degrees</i>

Table 3: Physical characteristics of the Sea King MK50 helicopter [2, 3, 13]

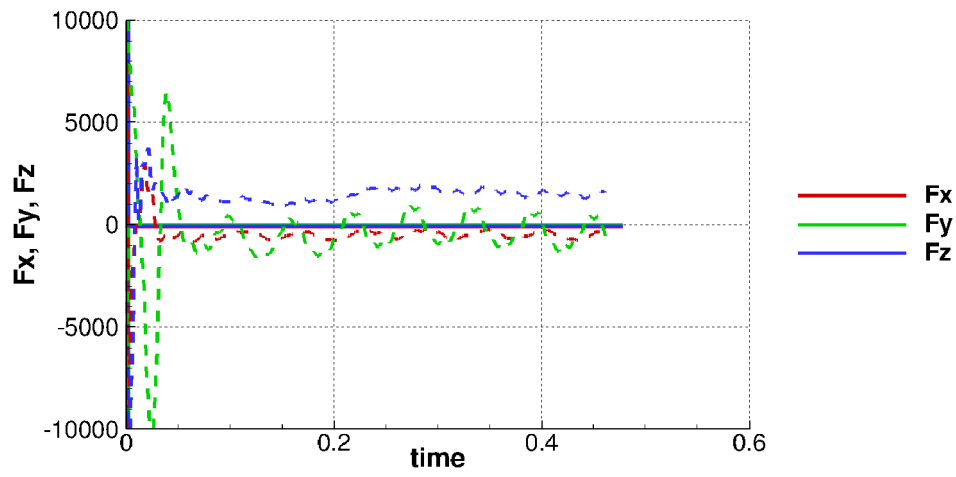


(a) Position and attitude

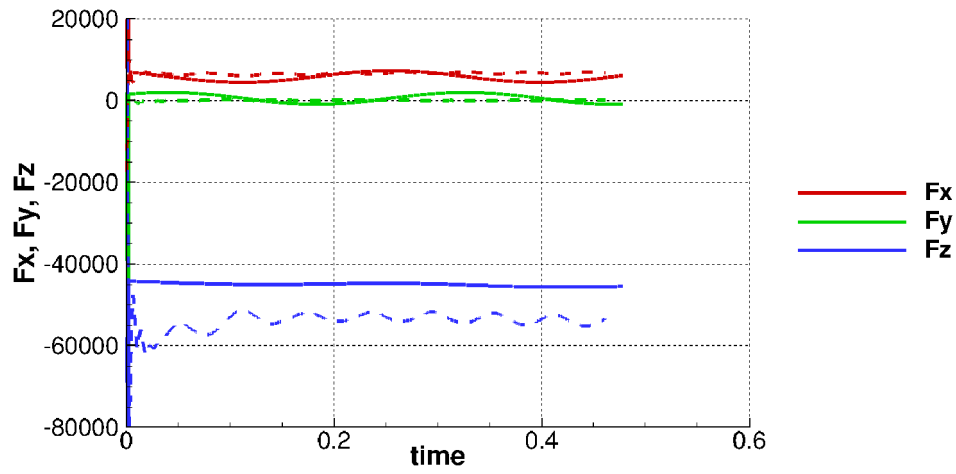


(b) Control angles

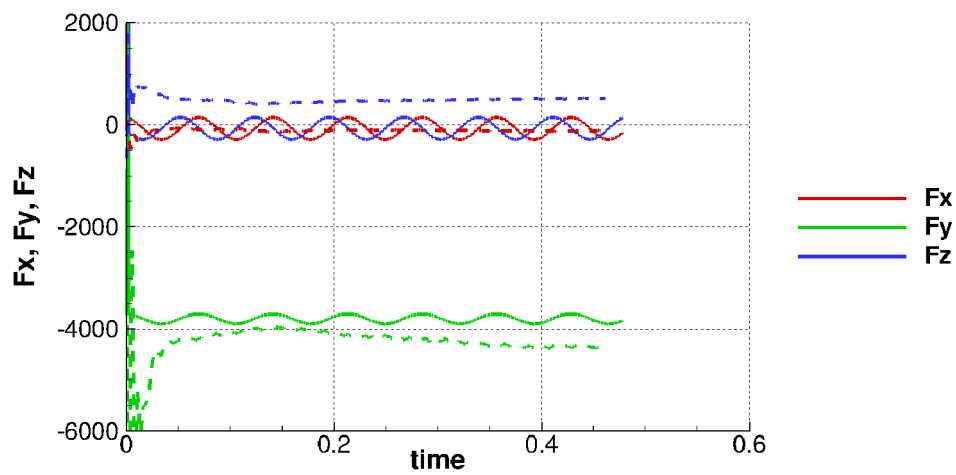
Figure 12: Aircraft position, attitude and control angles predicted using inverse modeling and obtained during LQR piloted simulation. Time is in seconds, control angles in degrees, distances in meters.



(a) Fuselage



(b) Main Rotor



(c) Tail Rotor

Figure 13: Comparison between HFM (solid line) and HMB (dashed line) loads on the fuselage, main rotor and tail rotor in trimmed forward flight. Loads are in Newtons.